NUMERICAL ANALYSIS OF A FRICTIONAL IMPACT OSCILLATOR

Giovanni Lancioni
Dep. of Architecture, Buildings and Constructions
Polytechnic University of Marche, Ancona
Italy
g.lancioni@univpm.it

Ugo Galvanetto
Department of Aeronautics
Imperial College London
United Kingdom
u.galvanetto@imperial.ac.uk

Stefano Lenci
Dep. of Architecture, Buildings and Constructions
Polytechnic University of Marche, Ancona
Italy
lenci@univpm.it

Abstract
The dynamics of a two-dimensional system constituted by two masses subjected to elastic, gravitational and viscous forces and constrained by a moving frictional mono-lateral surface is investigated numerically by means of a self-made code. The model, capable of reproducing the hopping phenomenon of a windscreen wiper, exhibits a time-varying dynamics which has a non-smooth nature due to the impact and friction and is affected by geometrical non-linearities. Various periodic motions are found and the dependence on the problem parameters, in particular on the friction coefficient, is investigated in detail.

Key words
Time varying system, non-smooth dynamics, stick-slip, impact, windscreen wiper.

1 Introduction

This communication presents the main results of a numerical study of the dynamics of the two-dimensional mass-spring-damper system depicted in Fig. 1 [Lancioni, Lenci and Galvanetto, 2007]. It consists of two rigid bodies of masses m_1 and m_2 immersed in a vertical downward gravitational field and constrained by elastic springs, by viscous dashpots and by a moving frictional mono-lateral surface. This model, called Frictional Impact Oscillator [Leine, Brogliato and Nijmeijer, 2002], reproduces the hopping phenomenon observed in many applications, such as the motion of a piece of chalk pushed over a blackboard or that of a robotic harm on a plane. The system can also be seen as a simplified model of the transverse section of a windscreen wiper blade moving on the glass of a car. k_φ represents the stiffness of the rubber cantilever in wiper blade, while k_y measures the stiffness of the wiper metal harm. The investigation of the dynamics is useful to understand the causes of the hopping and, as a result, to suggest the appropriate remedies to avoid this unwanted motion.

The proposed model can be classified as a time varying system, because its dynamics is divided in three different regimes: free-flight, slipping or sticking of the mass m_1. Each motion is characterized by a different number of degrees of freedom, two, one and zero, respectively. The resulting equations of motion are complemented by appropriate transitions laws from one regime to the next. In particular, for the impact of the m_1 on the surface, we adopt the Poisson's law proposed in [Pfeiffer and Glocker, 1996] and analysed in detail in [Pfeiffer and Foerg, 2005], where the introduction of restitution impulses allows for the bouncing of mass m_1. The perfectly plastic impact law considered in [Lancioni, Lenci and Galvanetto, 2007] is obtained as a particular case when the normal restitution coefficient is set equal to zero.

The dynamics of the model are very intricate as a consequence of the geometric nonlinearity in the motion of the mass m_1, of the Coulumb dry friction for the contact of m_1, and of the impact law. As analytical solutions are possible only in a limited number of cases, a numerical approach is pursued by means of a self-made code.

We investigate the effects of the impact law on the system dynamics by considering a completely inelastic impact as well as a partially elastic impact. The dynamical behaviours of these two cases are studied for different values of the frictional coefficient. Completely different dynamics have been found, and their correspond-

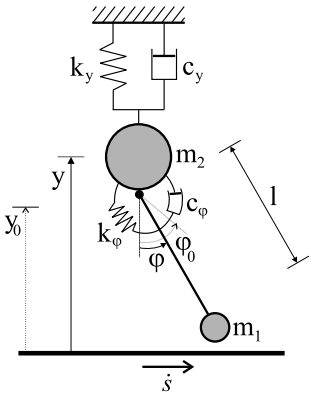

Figure 1. Frictional Impact Oscillator.

ing bifurcation branches are connected by smooth and non-smooth bifurcation points. Finally, some simulations are performed by considering a sinusoidal belt velocity to reproduce the motion of a windscreen wiper.

2 Regimes of motion and transition laws

We summarize in this Section the equations which govern the motion and the transition from one regime to the other, and we refer to [Lancioni, Lenci and Galvanetto, 2007] for an extended treatment and an in-depth discussion. For the two-mass system represented in Fig. 1, the parameters chosen to describe the motion are the rotation φ of the rigid bar connecting m_1 and m_2, and the distance y of m_2 from the surface. The normal and tangential contact forces between the mass m_1 and the moving surface are λ_N and λ_T, respectively. The problem unknowns φ, y, λ_N and λ_T are determined by the equations of motion

$$\begin{bmatrix} m_1 l^2 & m_1 l \sin\varphi \\ m_1 l \sin\varphi & m_1 + m_2 \end{bmatrix} \begin{bmatrix} \ddot{\varphi} \\ \ddot{y} \end{bmatrix} = \begin{bmatrix} l\sin\varphi & l\cos\varphi \\ 1 & 0 \end{bmatrix} \begin{bmatrix} \lambda_N \\ \lambda_T \end{bmatrix} - \begin{bmatrix} c_\varphi \dot{\varphi} + k_\varphi(\varphi - \varphi_0) + m_1 g l \sin\varphi \\ c_y \dot{y} + k_y(y - y_0) + m_1 l(\dot{\varphi})^2 \cos\varphi + (m_1 + m_2) g \end{bmatrix} \tag{1}$$

and by the contact law between m_1 and the sliding surface. In (1) g is the acceleration of gravity, while φ_0 and y_0 define the configuration of unstressed springs.

The three different regimes of motion, and the contact law between m_1 and the surface, which provides the two missing equations, are modeled as follows. Let $g_N = y - l\cos\varphi$ be the distance between m_1 and the surface, and let $\dot{g}_T = l\dot{\varphi}\cos\varphi - v$ (here $v = \dot{s}$ is the velocity of the surface, see Fig. 1) be the relative horizontal velocity. Note that $g_N < 0$ is not allowed by the impenetrability condition of the moving surface.

2.1 Free-flight

In this case the mass m_1 is detached from the surface. The contact forces vanish, $\lambda_N = \lambda_T = 0$, and the motion is determined by solving system (1) with respect to φ and y. Condition of existence of this regime is $g_N > 0$.

2.2 Contact regimes

In the next two regimes, m_1 is in contact with the surface. The contact conditions are $g_N = \dot{g}_N = \ddot{g}_N = 0$, and allows to write y and its derivatives in terms of the variable φ:

$$\begin{aligned} y &= l\cos\varphi, \qquad & \dot{y} &= -l\dot{\varphi}\sin\varphi, \\ \ddot{y} &= -l(\dot{\varphi})^2\cos\varphi - l\ddot{\varphi}\sin\varphi. \end{aligned} \tag{2}$$

Thus, y is no longer an unknown in these regimes. The Coulumb friction law governs the behaviour in the tangential direction and defines two possible situations: slip or stick.

2.2.1 Slip In this case the relative tangential velocity is not null. If $\dot{g}_T > 0$, then $\lambda_T = -\mu\lambda_N$ (positive slip, μ is the Coulumb friction coefficient) and if $\dot{g}_T < 0$, then $\lambda_T = +\mu\lambda_N$ (negative slip). The remaining variables and φ and λ_N are determined by (1).

2.2.2 Stick In this case the relative tangential velocity is null, $\dot{g}_T = 0$, the system has no more degrees of freedom, and its dynamics is completely determined by the motion of the surface. Equations (1) are used to evaluate the contact forces λ_N and λ_T, which have to satisfy the condition $|\lambda_T| \leq \lambda_N$, which is the condition of existence of this regime.

2.3 Transition laws

The transition from one regime to the other is governed by the following conditions: the slip motion passes to stick when $\dot{g}_T$ becomes equal to 0; the opposite transition from stick to (negative/positive) slip occurs when λ_T becomes equal to $\pm\mu\lambda_N$; the mass m_1 detaches when $\lambda_N = 0$ and the motion moves from slip or stick to free-flight.

The transition from free-flight to other regimes is governed by the Poisson's impact law [Pfeiffer and Glocker, 1996; Lancioni, Lenci and Galvanetto, 2007]. Within the infinitesimal time interval $[t_0, t_2]$ of an impact, we distinguish two phases: a phase of compression $[t_0, t_1]$ and a phase of expansion $[t_1, t_2]$. The Poisson law states that normal impulse in the expansion phase is $\Lambda_{Ne} = \varepsilon_N \Lambda_{Nc}$, where Λ_{Nc} is the impulse in the compression phase and $\varepsilon_N \in [0, 1]$ is the restitution coefficient. When $\varepsilon_N = 0$, the impact is perfectly plastic, as assumed in [Leine, Brogliato and Nijmeijer, 2002]. The impact laws are obtained by integrating the motion equations (1) within the compression and

expansion time intervals and their detailed expressions are given in [Lancioni, Lenci and Galvanetto, 2007]. We just notice here that for $\varepsilon_N > 0$ the mass m_1 always bounces and the transition to the laid regimes happens through a "chattering" process [Demeio and Lenci, 2006]. In the numerical code we conventionally end the chattering when the time distance between two consecutive impacts is smaller than a given tolerance.

3 Numerical simulations

Here we show only few numerical results. A more extended set of simulations is reported in [Lancioni, Lenci and Galvanetto, 2007]. We consider two different impact laws: a fully inelastic impact by setting $\varepsilon_N = 0$, and a partially elastic impact by setting $\varepsilon_N = 0.2$. The dynamics of the two models are analysed by varying the dry friction coefficient μ. The other parameters are [Leine, Brogliato and Nijmeijer, 2002]: $m_1 = 0.1kg$, $m_2 = 1kg$, $l = 1m$, $k_y = 100N/m$, $k_\varphi = 100Nm$, $c_y = 10N/(ms)$, $c_\varphi = 0$, $\varphi_0 = \pi/8$, $y_0 = 1m$.

Fig. 2 reports the bifurcation diagrams of the maximum angular velocity $\dot{\varphi}_{max}$ as function of μ. The Poincaré maps are determined by considering the intersection of the trajectory with the surface $\dot{\varphi} = 0$ when $\ddot{\varphi} > 0$.

For small values of μ we observe only an equilibrium branch in a slip mode. By increasing μ, the equilibrium undergoes an Hopf bifurcation at $\mu = 0.40977$, after which a periodic oscillation in slip mode appears (see Fig. 2(b)). The equilibrium point for $\mu = 0.3$ and the periodic oscillation for $\mu = 0.4098$ are reported in Fig. 3. At $\mu = 0.40983$ the slip periodic branch disappears and the dynamics jump on another branch of solutions. This branch involves free-flight and impacts, and thus the path for $\varepsilon_N = 0$ is different from that for $\varepsilon_N = 0.2$. It is worth to note how the transition from contact motions to detached motions occurs through a hysteretic loop (see Fig. 2(b)), which is defined by the region of coexistence of the two solutions. In the case $\varepsilon_N = 0.2$, the detached motion consists of a sequence of periodic bounces of m_1 on the moving surface. Its orbit is denoted as "bouncing" in Fig. 3(a).

In the case $\varepsilon_N = 0$, an interesting phenomenon is observed near the bifurcation point at $\mu = 0.38957$ (see Fig. 2(c)). For decreasing μ, the solution is periodic of the type free flight-slip-stick-slip up to $\mu = 0.38965$. Here, in one "period" the stick phase between the two slip phases disappears, while it remains in the subsequent "period". Thus, the solution is now of the type free flight-slip-free flight-slip-stick-slip, and doubles its real period. At a lower value of μ the stick phase disappears from two consecutive periods, and so on. A cascade of these events occurs, in each of which the motion periodicity increases of one, as well as the number of consecutive "periods" without stick phase. The generic period i motion is constituted by $i - 1$ free flight-slip cycles and 1 free flight-slip-stick-slip cycle. These events accumulate on the final (bifurcation) point, which corresponds to a motion with an infinite period, and cause the disappearance of the residual attractor.

For increasing values of μ the motion is periodic of the type free flight-stick-slip up to $\mu = 6450$ and of the type free flight-stick for $\mu > 6450$.

We now set $m_1 = 0.4kg$ and $k_\varphi = 25Nm$, a case in which the geometrical non-linearity plays a more important role on the system dynamics. The bifurcation diagrams are reported in Fig. 4. In this case, the diagrams obtained with $\varepsilon_N = 0$ and $\varepsilon_N = 0.2$ practically coincide, also in the regions where there is free-flight. The bifurcation curve is constituted by four branches related to four different dynamical behaviors. The branch $\mu < 0.353$ is an equilibrium branch. The next three branches correspond to periodic motions: for $0.353 < \mu < 0.360$ the motion is an oscillation in slip mode, for $0.360 < \mu < 0.453$ the periodic oscillation involves also the stick mode, and for $\mu > 0.453$ a more complex free flight-slip-stick-slip motion takes place. In Fig. 4(b) the bifurcation diagram is enlarged in correspondence of the slip oscillating branch. The smooth transition from equilibrium to periodic slip motion is a Hopf bifurcation occurring at $\mu = 0.353$. The orbits in the $\varphi - \dot{\varphi}$ phase space are reported in Fig. 5 for different values of μ, where we observe that the larger is μ the larger is the diameter of the orbits. The motion experiences impacts only for $\mu > 0.453$, and, as a result, only in this region the periodic motion depends on the impact law. However the orbits for $\varepsilon_N = 0$ and $\varepsilon_N = 0.2$ practically coincide since in the case of $\varepsilon_N = 0.2$ the chattering process through which the motion passes from free-flight to slip happens in a very short time interval.

We now consider a sinusoidal surface velocity of the form $v = sin(\pi t/2)$ since our aim is to reproduce the motion of windscreen wipers and to investigate the hopping phenomenon, which usually takes place when φ and v have opposite signs and produces undesired noise and marks on the glass, reducing the visibility. To analyze the influence of the friction on the hopping motion, two simulations are performed with $\mu = 0.5$ and $\mu = 0.3$, respectively, and the results are shown in Fig. 6. We mainly observe that the hopping occurs only for $\mu = 0.5$. In this case, when $v < 0$, the motion is essentially in free-flight with short slip periods. These simulations reveal the well known fact that a large value of the friction coefficient facilitates the hopping phenomenon. In fact, according to common sense, in the case of a windscreen wiper, the hopping occurs when the glass is dirty and dry, i.e., when μ has a large value.

4 Conclusion

Numerical simulations of the Frictional Impact Oscillator reported in Fig. 1 have been reported with the aim of highlighting the main aspect of its nonlinear dynamics.

Both cases of constant and harmonic velocity of the moving surface are considered. The former is that classically used in the literature, and permits to study in a simpler way the most common bifurcations of the system dynamics. The latter, on the other end, is more close to the real applications, such as, for example, the windscreen wiper, which actually motivate this study.

Various smooth and non-smooth bifurcations of equilibrium points and of periodic orbits have been detected and illustrated by the combined use of bifurcation diagrams and of phase portrait. An apparently new period-adding phenomenon has been detected.

Acknowledgements

This work has been developed in the framework of the International Research Project "Dynamics and control of engineering systems affected by friction forces" founded by the Royal Society of London.

References

Demeio, L. and Lenci, S. (2006) Asymptotic analysis of chattering oscillations for an impacting inverted pendulum, *Quart. J. Mech. Appl. Math.*, **59**, pp. 419–434.

Lancioni, G., Lenci, S. and Galvanetto, U. (2007) Nonlinear dynamics of a mechanical system constrained by a frictional mono-lateral surface. *Submitted.*

Leine, R., Brogliato, B. and Nijmeijer, H. (2002) Periodic motion and bifurcations induced by the Painlevé paradox. *Eur. J. of Mechanics A/Solids*, **21**, pp. 869–896.

Pfeiffer, F. and Glocker, C. (1996). *Multibody dynamics with unilateral contacts*. John Wiley & Sons, Munich.

Pfeiffer, F. and Foerg, M.O. (2005) On the structure of multiple impact system. *Nonlinear Dynamics*, **42**, pp. 101–112.

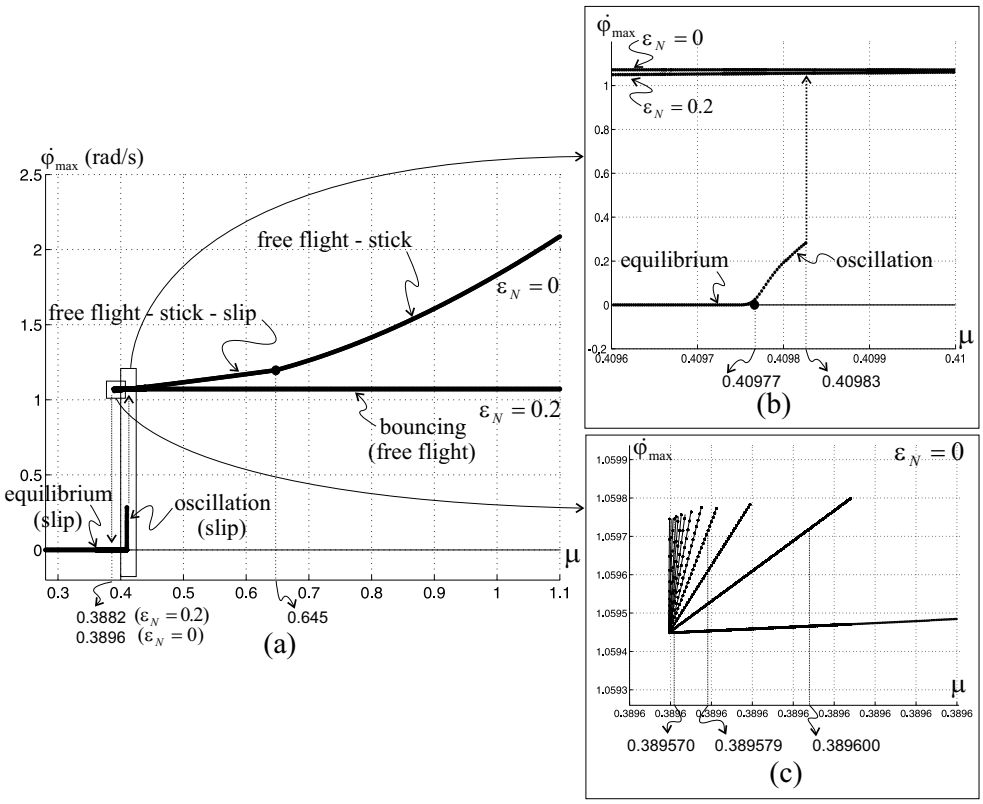

Figure 2. Bifurcation diagrams.

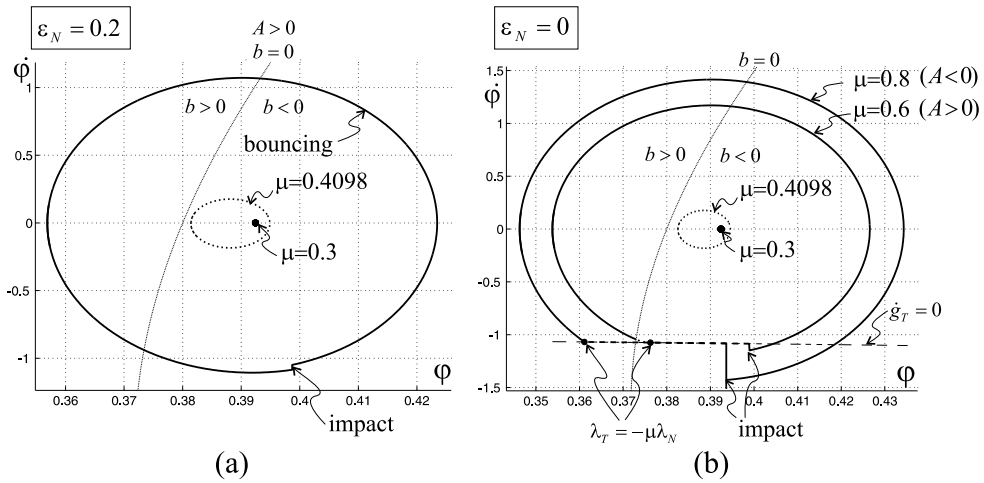

Figure 3. Orbits in the $\varphi - \dot{\varphi}$ plane. Free-flight ≡ solid line; slip ≡ dotted line; stick ≡ dashed line.

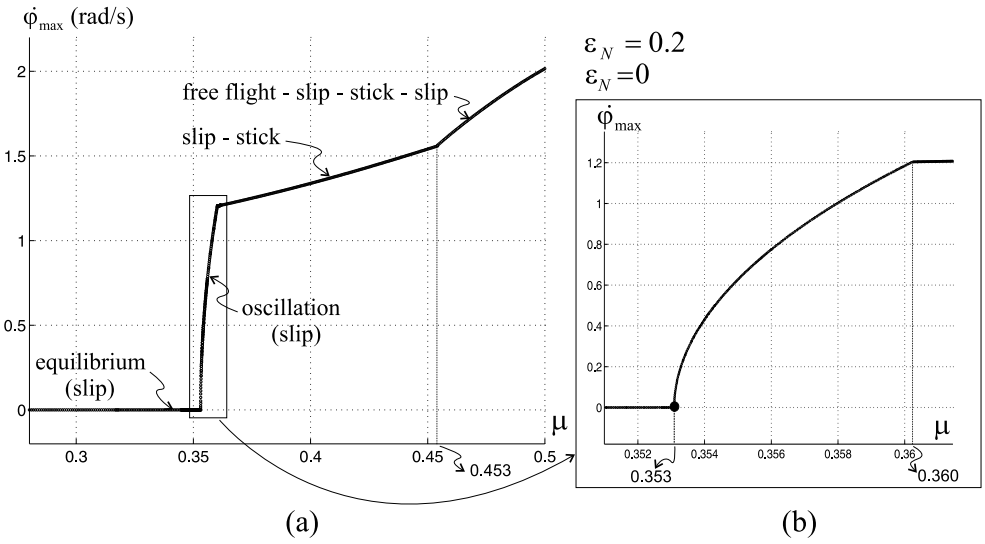

Figure 4. Bifurcation diagrams in the case $m_1 = 0.4kg$ and $k_\varphi = 25Nm$.

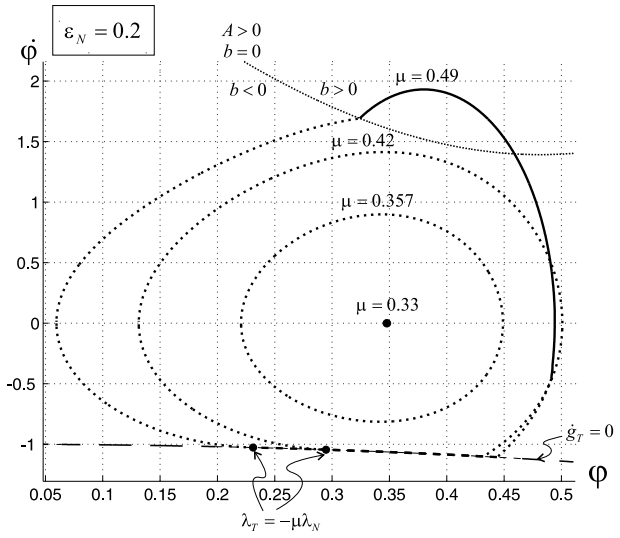

Figure 5. Orbits in the $\varphi - \dot{\varphi}$ plane in the case $m_1 = 0.4kg$ and $k_\varphi = 25Nm$. Free-flight $\equiv$ solid line; slip $\equiv$ dotted line; stick $\equiv$ dashed line.

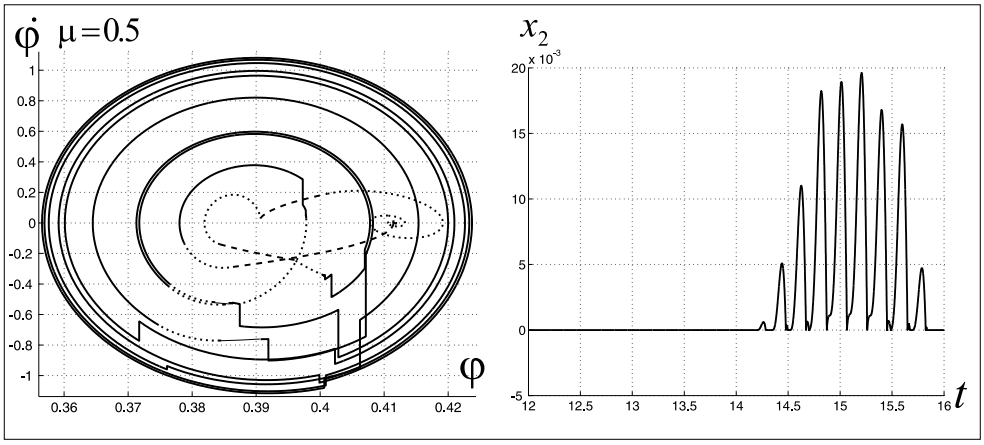

(a)

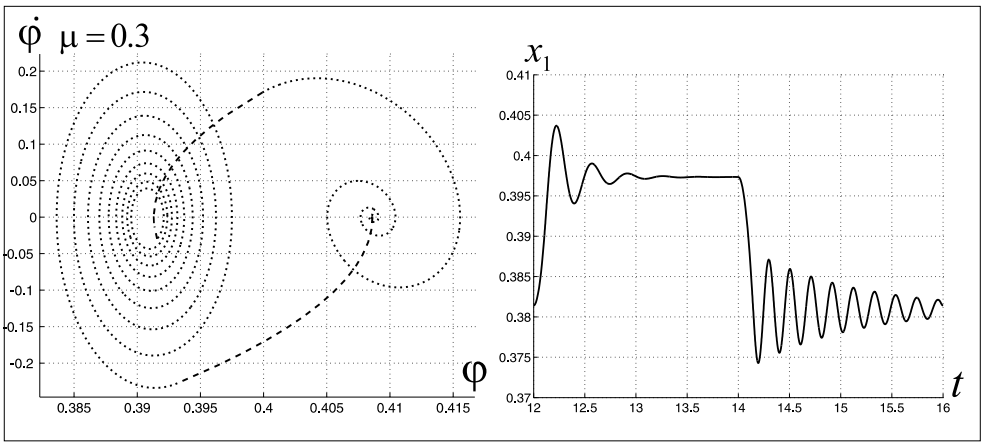

(b)

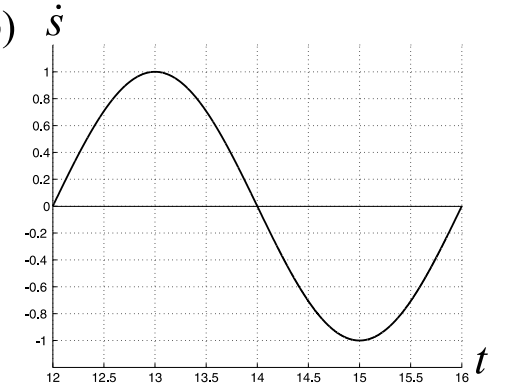

Figure 6. Sinusoidal surface velocity. Phase portraits and time histories for $\mu = 0.5$ and $\mu = 0.3$.